Siloxene: Chemical Quantum Confinement Due to Oxygen in a Silicon Matrix

Peter Deák,[a] Martin Rosenbauer, Martin Stutzmann, Jörg Weber, and Martin S. Brandt
Max-Planck-Institut für Festkörperforschung, Heisenbergstrasse 1, D-7000 Stuttgart 80, Germany
(Received 10 April 1992)

Siloxene ($Si_6O_3H_6$) and its derivatives show strong visible luminescence. By applying semiempirical quantum chemical calculations to the siloxene structure, we demonstrate that the presence of oxygen in a planar array of silicon atoms results in molecular orbitals confined to Si rings or chains which are responsible for the luminescence properties. Our results on the optical and vibrational properties of siloxene support earlier experimental results identifying siloxenelike structures as the luminescent agent in porous silicon.

PACS numbers: 61.40.+e, 71.25.Tn, 78.55.Hx

The recently discovered strong visible luminescence in anodically etched, porous silicon [1, 2] is generally attributed to quantum size effects: optical transitions are assumed to occur in small silicon crystallites or "quantum wires" produced during etching. Based on the similarity of the infrared and luminescence spectra of porous silicon with those of a particular class of Si–O–H compounds derived from siloxenes ($Si_6O_3H_6$), however, it has recently been proposed that the visible luminescence of porous silicon originates from substituted siloxene [3, 4]. In this paper, calculations on the electronic structure of siloxene are presented, showing that the particular optical properties of this compound are due to linear chains and/or sixfold rings of Si atoms isolated from each other by ordered insertion of oxygen atoms into a planar array of silicon atoms. While the electronic states in the assumed quantum wires of porous silicon would be confined physically due to the geometrical "quantum size" of the small columnar silicon crystallites, the confinement in siloxene can be linked with the chemical composition. The calculated optical properties fit well to the experimental ones observed for both siloxene and porous silicon. In addition, our calculations provide a basis for the assignment of the different vibrational bands in siloxene. Given the almost identical vibrational spectra of siloxene derivatives and many strongly luminescing porous silicon samples we argue that "chemical confinement" due to oxygen should be considered as a possible explanation for the luminescence in porous silicon as well.

Siloxene, and its derivatives, have long been known in silicon chemistry because of their outstanding color and luminescence properties [5–7]. The structure of "as prepared" siloxene [8, 9] consists of the layers shown in Fig. 1(a), stacked on top of each other. The silicon atoms form a biplanar array, similar to that of a (111) double layer in *c*-Si (the lattice constant in the layers is 3.83 Å, very close to that in crystalline Si). The remaining valences of the silicon atoms are alternatingly saturated by H atoms and OH groups. Upon heat treatment, siloxene may undergo structural transformations resulting in the loss of long-range order. The arising structure is probably a mixture of the original one [Fig. 1(a)] and the one shown in Fig. 1(c) [10] or, possibly, the one in Fig. 1(b), although only little experimental evidence exists for the latter two. In the structures of Figs. 1(b) and 1(c) the oxygen atoms are inserted into the Si planes and the remaining valences of the Si atoms are saturated—in the ideal case—entirely by hydrogen. The substitution of these hydrogen atoms by other monovalent radicals is assumed to be responsible for the tuning of the color and fluorescence of siloxene derivatives over a large spectral range [6] (see the right-hand side of Table I for the spe-

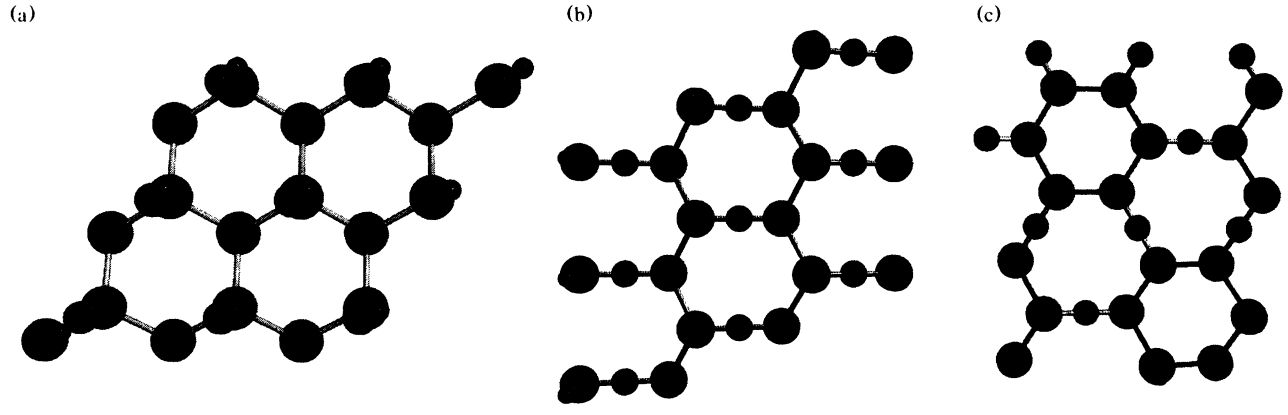

FIG. 1. Different modifications of siloxene: (a) $[Si_2H(OH)]_{3n}$ (planes), (b) $[Si_2H_2O]_{3n}$ (chains), and (c) $[Si_6H_6O_3]_n$ (sixfold Si rings). Si, O, and H atoms are marked by green, blue, and red spheres, respectively.

TABLE I. Calculated optical properties (in eV) of OH-substituted siloxene in the ring configuration, $[Si_6H_{6-x}(OH)_xO_3]_n$. $E_g(\overline{\Gamma})$ and $E_g(\overline{K})$ are the first direct transitions (between the states $\sigma[\Gamma] - \pi[\Gamma]$ and $\sigma[\overline{K}] - s^*[\overline{K}]$, respectively), while E_0 is the indirect gap. The transition with the highest oscillator strength (not listed) changes from 4.42 to 3.45 eV. The experimentally observed fluorescence properties [6] are shown in the last column.

x	$E_g(\overline{\Gamma})$	$E_g(\overline{K})$	$E_0(\overline{\Gamma} - \overline{K})$	Fluorescence	
0	4.15	3.50	2.84	not visible	≥ 3.0 eV
1	4.01	3.25	2.67	yellow-green	≈ 2.5 eV
2	3.92	3.07	2.52	orange	≈ 2.2 eV
3	3.87	2.94	2.38	red	≈ 1.9 eV
6	3.77	2.31	1.82	dark red	≈ 1.6 eV

cial case of substitution with OH radicals). The structures in Figs. 1(b) and 1(c) consist of periodic arrays of Si chains and Si rings, respectively, linked—or rather separated from each other—by oxygen atoms.

We have modeled the siloxene structures $[Si_2H(OH)]_{3n}$ (planes), $[Si_2H_2O]_{3n}$ (chains), and $[Si_6H_6O_3]_n$ (rings) shown in Fig. 1, as well as the chemical derivatives of the last one obtained by H→OH substitution, $[Si_6H_{6-x}(OH)_xO_3]_n$ (x = 1, 2, 3, and 6). We use cyclic clusters containing n = 3 or n = 4 units, representing various (discrete) samplings of special wave vectors in the 2D hexagonal Brillouin zone (BZ). Details of the cyclic cluster model are given elsewhere [11]. We have employed a variety of particularly suited semiempirical methods to calculate the equilibrium geometry, relative stability, electronic transitions, and vibrational frequencies of these structures. The applicability of these basically "chemical" approximations to solid-state studies has been tested in crystalline silicon [11] and α-quartz [12]. For example, these methods have been successfully applied to predict the behavior of hydrogen [13] and oxygen complexes [14] in c-Si, as well as surface reconstruction and adsorption phenomena [15, 16]. Since the long-range order in the experimentally studied siloxene samples appears to be strongly limited, the application of these methods is also justified in the present case. Among the various semiempirical methods available, MINDO/3 (modified intermediate neglect of differential overlap) has been found to give the most reliable geometries in silicon based systems [11, 17]. Since MINDO/3 is known to underestimate the strength of Si-Si and overestimate the strength of Si-O bonds, we have performed calculations also by using the AM1 (Austin model) method which is more reliable in predicting bond strengths and force constants. Since none of the above methods is suitable to describe the conduction band of c-Si, the spectroscopic version of CNDO (complete neglect of differential overlap), CNDO/S was used to calculate the electronic transitions at the equilibrium geometry. (For more references about semiempirical methods see [11].)

The MINDO/3 and AM1 methods result in essentially identical geometries for each of the three structures (shown in Fig. 1). The nearest-neighbor Si-Si distances given by MINDO/3 are 2.437 Å, 2.447 Å, and 2.438 Å in the planes, in chains, and in rings, respectively (compared to 2.441 Å calculated for bulk c-Si). In establishing the relative stability of these structures, one has to be aware of the fact that the accuracy of calculated total energies can only be the same if the systems contain the same number of each of the different bonds. The energy change upon the transformation of the plane structure into either the chain or the ring structure arises from changing the number of bonds (one Si-Si and one O-H bond is broken, and one Si-O and one Si-H bond is created for every pair of silicon atoms) and from the subsequent relaxation of the electrons and nuclei. Even relatively small errors in the individual binding energies may accumulate substantially in such a case. The errors in the individual binding energies can be estimated by comparing calculated and experimental bond dissociation energies of appropriate molecules. Taking these into account, the energy gain on the transformations of plane → chain and plane → ring can be estimated to be 0.90 and 0.94 eV/Si-pair, respectively, by MINDO/3 and 0.26 and 0.62 eV/Si-pair by AM1. Consequently, the plane structure is definitely metastable, and heat treatment should transform it into a more disordered structure consisting of a mixture of the three structures shown in Fig. 1. This is indeed observed experimentally [4, 9].

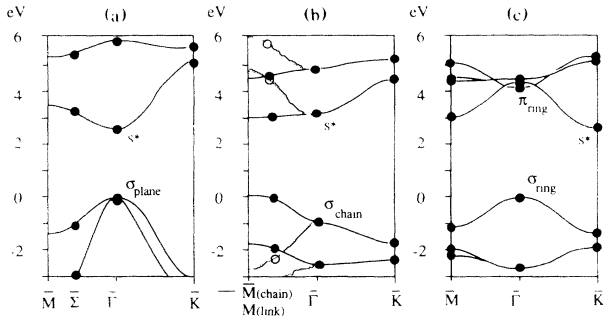

FIG. 2. The CNDO/S electronic structures of (a) $[Si_2H(OH)]_{3n}$, (b) $[Si_2H_2O]_{3n}$, and (c) $[Si_6H_6O_3]_n$ around the fundamental gap (only dots are calculated values). The solid lines between $\overline{\Gamma}$ and $\overline{M}$ in (b) show the bands along chain directions. The dotted lines correspond to bands along the interlink between chains.

The electronic structures calculated by CNDO/S using the geometry supplied by MINDO/3 are shown in Fig. 2 for all three modifications. The cyclic cluster calculations result in one-electron eigenvalues at discrete wave vectors of the hexagonal BZ. Those belonging to the center of the hexagon ($\overline{\Gamma}$), to the corners ($\overline{K}$), and to those between $\overline{\Gamma}$ and the midpoint of the border line ($\overline{M}$) are shown. The BZ of the chain structure [Fig. 1(b)] is an irregular hexagon: here the bands in the direction of both $\overline{M}$ points are shown. The calculated values are represented by dots; the "bands" are interpolated using sim-

ple symmetry and compatibility relations only in order to facilitate evaluation.

For the Si planes, $[Si_2H(OH)]_{3n}$, the top of the valence band (VB) is at $\overline{\Gamma}$: the corresponding orbital (σ_{plane}) is a bonding combination of Si $3p_x$ and $3p_y$ orbitals extending over the whole planar array of Si atoms. The lowest subband in the conduction band (CB) consists of antibonding states with predominantly Si $3s$ character (s^*). The whole electronic structure is very similar to that of planar polysilane, $[Si_2H_2]_n$, calculated by Takeda and Shiraishi [18] within the local-density-functional approximation. An apparent difference is that our calculation results in a direct gap of 2.73 eV at $\overline{\Gamma}$, while an indirect gap between $\overline{\Gamma}$ and $\overline{\Sigma}$ was reported in [18] with the first direct transition at $\overline{\Gamma}$ being 0.15 eV higher. We calculate the first transition energy from the top of the VB at $\overline{\Gamma}$ to the CB at $\overline{\Sigma}$ to be 3.21 eV, i.e., 0.48 eV higher than the direct gap. This is, however, likely to be an effect of the neglect of atomic orbital overlaps in the semiempirical methods, overestimating the stability of the purely s-type state at $\overline{\Gamma}$ with respect to the state at $\overline{\Sigma}$ having a considerable Si $3p$ admixture. Therefore, it is possible that the siloxene structure with Si planes [Fig. 1(a)] has an indirect gap as well. Efficient optical excitation should be expected above 3.2 eV.

In the chain modification, $[Si_2H_2O]_{3n}$, the gap is direct, but it is shifted away from $\overline{\Gamma}$ in direction of a $\vec{k}$ vector parallel to the Si chains. The first transition has an energy of 2.95 eV. The bottom of the CB is still an extended s^* orbital, but the top of the VB (σ_{chain}) is now a bonding combination of Si $3p_x$ orbitals along chain directions. Two neighboring chains are antibonded, so that the bridging O atoms are in a nodal plane. The electrons in these orbitals are confined to the Si chains. The Si-O-Si bridges between the chains give rise to a much larger splitting between bonding and antibonding states [dotted lines in Fig. 2(b)] and in effect act as an electronic barrier between the chains which can thus be regarded as "quantum wires." Therefore, the chain configuration of siloxene should exhibit electronic properties similar to linear polysilane, $(SiH_2)_n$, which is also a compound known to show efficient visible luminescence.

For the siloxene configuration containing sixfold silicon rings, $[Si_6H_6O_3]_n$, the gap is again indirect. The energies of the optical transitions can be seen in the first row of Table I (unsubstituted case). Figure 3 shows the probability distribution in the orbital at the top of the VB, $\sigma_{\text{ring}}(\overline{\Gamma})$. This orbital consists of Si $3p_x$-$3p_y$ hybrids in σ-bonded combinations around the rings. The Si-O-Si antibond between the rings leads to a confinement of the electrons in these rings, giving rise to a molecular "quantum dot"-like behavior. The degree of localization can be judged from the dispersion (1.1 eV) which is about the same as that of the bands in quartz [12]. The orbitals around the bottom of the CB are of extended s^* type, while at $\overline{\Gamma}$ it is a π-bonded combination of $3p_x$-$3p_y$ hybrids around the rings and with Si–O–Si antibonds between the rings.

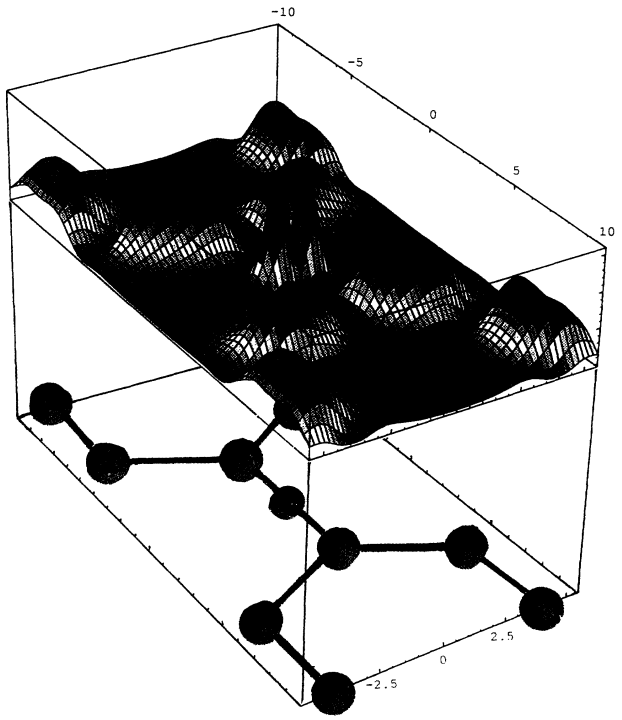

FIG. 3. Three-dimensional plot of the probability distribution of the electrons in the highest occupied orbital (σ_{ring}) confined to Si_6 rings at the top of the VB in $[Si_6H_6O_3]_3$ (ring structure). The two sharp peaks in the center of the plot are due to oxygen $2p$ electrons. Note the low electronic density between Si and O in the Si–O–Si direction (in a.u.).

The electronic structure of the different idealized siloxene modifications provides a semiquantitative explanation of the observed optical properties of siloxene and should also be considered for the explanation of the visible luminescence seen in porous silicon. Thus, efficient excitation of electron-hole pairs can be achieved at the energies of the two lowest direct transitions, which are expected around 2.6 eV and between 3.0 and 3.9 eV for siloxene derivatives luminescing in the red. This compares reasonably well to the experimental energies of 2.4 and 3.2 eV obtained from photoluminescence excitation spectra of both siloxene and porous silicon [3, 4]. Radiative band-to-band recombination, on the other hand, occurs at much lower energies. Thus, the large *apparent* Stokes shifts observed in porous silicon as well as in siloxene (typically of the order of 0.5–1 eV), can be explained readily by recombination of optically excited, localized carriers at the lowest transition energy of the indirect gap between $\sigma(\overline{\Gamma})$ and $s^*(\overline{K})$. Such an assumption is in agreement with the observation that the *actual* Stokes shift in siloxene is less than 0.3 eV [19] and also explains the long radiative lifetimes observed in both siloxene and porous silicon [4].

Substituting the H terminators of the Si atoms with more electronegative radicals (such as OH) will diminish

the electron population in the bonding orbitals around the Si rings, thus weakening the bond and decreasing the bonding–antibonding splitting. As a result both the direct and the indirect gap (left-hand side of Table I) decrease. The calculated values are well in the range observed for both siloxene and porous silicon [4], especially since no Stokes shift has been taken into account. The calculated Stokes shift in the indirect band-to-band transition due to atomic relaxations localizing the electron-hole pair is 0.06 eV for the unsubstituted ring and 0.11 eV for $[Si_6H_3(OH)_3O_3]_n$ (to be subtracted from the values in Table I).

Besides the optical properties, the vibrational spectra of porous silicon and siloxene are also very similar [4]. We have used the AM1 approximation to calculate the vibrational spectrum for the siloxene structures with planes and with (unsubstituted) rings. The calculated Si-H stretching mode frequencies at $\overline{\Gamma}$ are 2211 cm^{-1} in the plane structure and between 2216 and 2210 cm^{-1} in the rings. It has been shown that the calculated Si-H stretching frequencies should and can be scaled linearly in order to compare them with experimental data [20]. For example, using the ratio of the calculated and the experimental Si-H stretching frequency of the $HSi(CH_3)_3$ molecule, the scaled AM1 frequency of the optical phonon mode, $\nu(\overline{\Gamma}_1)$, in a hydrogen covered Si(111) surface is 2076 cm^{-1}, to be compared with the experimentally observed 2083 cm^{-1}. Using the same scaling factor, the Si-H frequencies in siloxene are 2105 cm^{-1} in the plane and between 2109 and 2104 cm^{-1} in the rings. The first value coincides with the experimentally observed band for "as prepared" siloxene (and the predominant band in porous silicon); however, the predicted increase upon heat treatment [transformation from Figs. 1(a) to 1(c)] does not explain the experimentally observed bands which develop at about 2180 and 2250 cm^{-1} [4]. These bands are due to further oxidation of the Si plane and do not occur in the ideal siloxene structures of Fig. 1. The highest Si-Si stretching mode vibration is calculated to be 478 cm^{-1} in the plane and 469 cm^{-1} in the ring structure. [The phonon frequency, $\nu(\overline{\Gamma}_{25'})$, for bulk Si is calculated to be 521 cm^{-1}, close to the experimental value, so no scaling is necessary in this case.] The predicted decrease from the plane to the ring structure is in line with the experimentally observed trend upon heat treatment (515 to 460 cm^{-1}; note that the observed frequencies also reflect possible selection rules in ordered structures) [4]. The most interesting result of our frequency calculation on the ring structure is that the Si–O–Si asymmetric stretching vibrations split into three phonon bands at $\nu(\overline{\Gamma}_1) = 1051$ and $\nu(\overline{\Gamma}_3) = 1114$ cm^{-1}. [For comparison, the calculated (observed) frequency in the disiloxane molecule is 1113 (1107) cm^{-1}.] The infrared spectra of both siloxene and porous silicon contain oxygen-related bands at about 1070 and 1160 cm^{-1} [4]. Upon heat treatment of siloxene, the two bands merge into a broad band around 1050 cm^{-1}, and the luminescence disappears. Our result indicates that these two bands are the consequence of the ordering of oxygen atoms which is responsible for the luminescence properties in the siloxene structure. Since the same bands appear in the spectrum of porous silicon which exhibits luminescence properties similar to siloxene, future work should address the question whether porous silicon also contains an ordered array of oxygen atoms.

In conclusion, we have shown that a regular array of oxygen atoms can isolate quantum wires and/or quantum dots in silicon. Provided all remaining dangling bonds are saturated by monovalent radicals, these low-dimensional structures exhibit optical and vibrational properties similar to those observed in porous silicon.

One of us (P.D.) acknowledges support from the A. von Humboldt Foundation and the Sonderforschungsbereich 91 at the University of Kaiserslautern. The authors would like to thank M. Cardona and H. J. Queisser for their support.

[a] Present address: Universität Kaiserslautern, Schrödingerstrasse 46, D-6750 Kaiserslautern, Germany. Permanent address: Technical University, Budapest H-1521, Hungary.

[1] L. T. Canham, Appl. Phys. Lett. **57**, 1046 (1990).
[2] V. Lehmann and U. Gösele, Appl. Phys. Lett. **58**, 856 (1991).
[3] M. S. Brandt, H. D. Fuchs, M. Stutzmann, J. Weber, and M. Cardona, Solid State Commun. **81**, 307 (1992).
[4] M. Stutzmann, J. Weber, M. S. Brandt, H. D. Fuchs, M. Rosenbauer, P. Deák, A. Höpner, and A. Breitschwerdt, Adv. Solid State Phys. **32**, 179 (1992).
[5] F. Wöhler, Liebigs Ann. Chem. **127**, 257 (1863).
[6] H. Kautsky and G. Herzberg, Z. Anorg. Allg. Chem. **139**, 135 (1924).
[7] E. Hengge, in *Silicon Chemistry II* (Springer, Berlin, 1974), p. 92.
[8] A. Weiss, G. Beil, and H. Meyer, Z. Naturforsch. **35B**, 25 (1979).
[9] H. Ubara, T. Imura, A. Hiraki, I. Hirabayashi, and K. Morigaki, J. Non-Cryst. Solids **59&60**, 641 (1983).
[10] H. Kautsky, W. Vogell, and F. Oeters, Z. Naturforsch. **10B**, 597 (1955).
[11] P. Deák and L. C. Snyder, Phys. Rev. B **36**, 9619 (1987).
[12] P. Deák and J. Giber, Phys. Lett. **88A**, 237 (1982).
[13] P. Deák, L. C. Snyder, and J. W. Corbett, Phys. Rev. B **37**, 6887 (1988).
[14] P. Deák, L. C. Snyder, and J. W. Corbett, Phys. Rev. B **45**, 11 612 (1992).
[15] P. Badziag, W. S. Verwoerd, and M. A. Van Hove, Phys. Rev. B **43**, 2058 (1991).
[16] B. I. Craig and P. V. Smith, Surf. Sci. **239**, 36 (1991).
[17] W. S. Verwoerd and K. Weimer, J. Comput. Chem. **12**, 417 (1991).
[18] K. Takeda and K. Shiraishi, Phys. Rev. B **39**, 11 028 (1989).
[19] I. Hirabayashi, K. Morigaki, and Sh. Yamanaka, J. Non-Cryst. Solids **59&60**, 645 (1983).
[20] P. Deák, L. C. Snyder, M. Heinrich, C. R. Ortiz, and J. W. Corbett, Physica (Amsterdam) **170B**, 253 (1991).

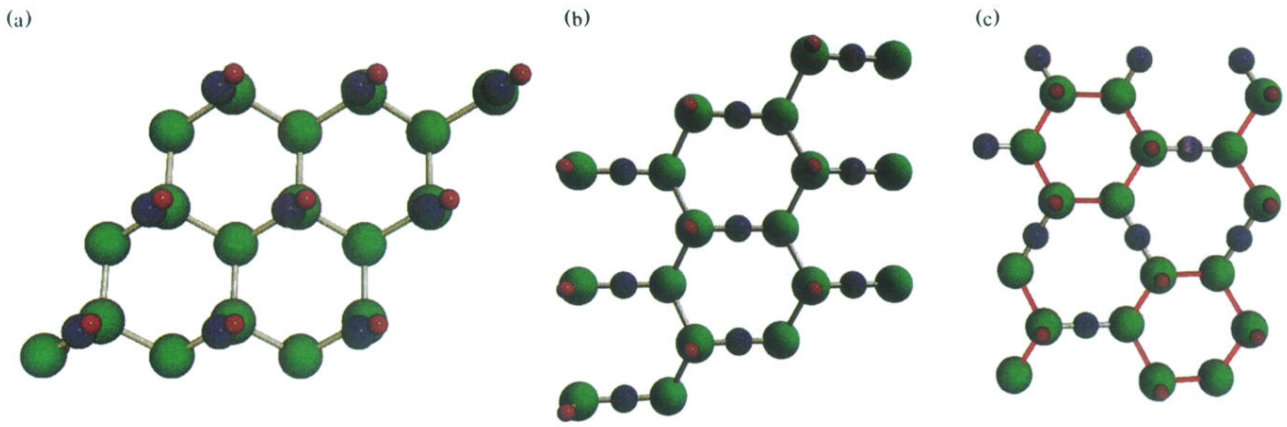

FIG. 1. Different modifications of siloxene: (a) $[Si_2H(OH)]_{3n}$ (planes), (b) $[Si_2H_2O]_{3n}$ (chains), and (c) $[Si_6H_6O_3]_n$ (sixfold Si rings). Si, O, and H atoms are marked by green, blue, and red spheres, respectively.

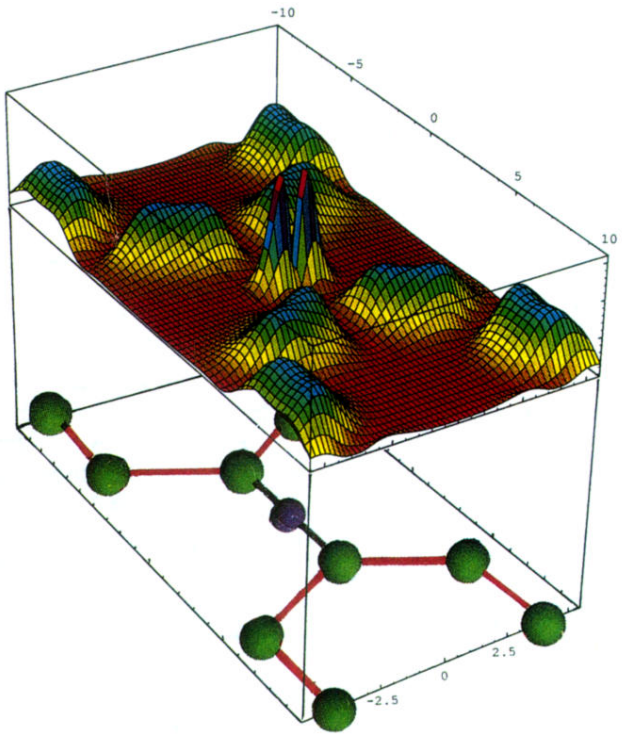

FIG. 3. Three-dimensional plot of the probability distribution of the electrons in the highest occupied orbital (σ_{ring}) confined to Si_6 rings at the top of the VB in $[Si_6H_6O_3]_3$ (ring structure). The two sharp peaks in the center of the plot are due to oxygen $2p$ electrons. Note the low electronic density between Si and O in the Si–O–Si direction (in a.u.).